Supporting Information

All-nanosheet OER/ORR bifunctional electrocatalyst for both aprotic and aqueous Li-O_2 batteries

Ming Zhang, *[a] Lu Zou,[b] Chunzhen Yang,[c] Yao Chen,[d] Zhongrong Shen,[a] and Bo Chi*[b]

[a]*CAS Key Laboratory of Design and Assembly of Functional Nanostructures, and Fujian Provincial Key Laboratory of Nanomaterials, Fujian Institute of Research on the Structure of Matter, Chinese Academy of Sciences, Fuzhou 350002, China*

[b]*Center for Fuel Cell Innovation, State Key Laboratory of Material Processing and Die & Mould Technology, School of Materials Science and Engineering, Huazhong University of Science &Technology, Wuhan, 430074, China*

[c]*The School of Materials, Sun Yat-sen University, Guangzhou, 510006, China*

[d]*The State Key Laboratory of Refractories and Metallurgy, Wuhan University of Science and Technology, Wuhan, 430081, China*

***Corresponding Author: E-mail: mingzhang@fjirsm.ac.cn (M Zhang); chibo@hust.edu.cn (B Chi)**

Contents

1. Materials and Methods

1.1 Materials

1.1.1 Synthesis of monolayer RuO_2 nanosheet

RuO_2 nanosheet was synthesized by elemental exfoliation of an ion-exchangeable layered potassium ruthenate (K-RuO_2) based on the literature with small modification.[1] Detail experiments are shown as following: Firstly, the layered K-RuO_2 precursor was synthesized via a solid-state reaction by calcination of a pelletized mixture of K_2CO_3 (393 mg) and RuO_2 (607 mg) at 850 °C for 12 h in tubefurance under a flow of argon gas. The product was ground into a fine powder and then washed with copious amounts of ultrapure water (Milli-Q, >18 MΩ cm). Proton-exchange of the interlayer potassium was conducted with 1 M HCl for 3 days at 60 °C to trigger the extraction of potassium ions, resulting in the layered ruthenic acid (H-RuO_2). The layered H-RuO_2 was added to a tetrabutylammonium hydroxide (TBAOH, 153 mg) aqueous solution (75 mL) under vigorously shaken for 10 days to exfoliate the layered H-RuO_2 into elementary RuO_2 nanosheets. Non-exfoliated impurity was removed by centrifugation at 2000 rpm for 30 min. Then, the as-exfoliated RuO_2 colloid was finally diluted to 1.0 (g-RuO_2) L^{-1} with ultrapure water. The colloidal suspension, which contains exfoliated, monolayered RuO_2 nanosheet, was used for further investigation.

1.1.2 Synthesis of Graphene oxide (GO)

GO was prepared by using modified Hummers method.[2] Briefly given as: 46 mL of 98 wt. % concentrated H_2SO_4 was cooled down below 0 ^oC in a 500 mL flask in ice bath for 30 min. Then, 2 g of graphite powder and 1.0 g of $NaNO_3$ was mixed together. This mixture was then added to cool concentrated H_2SO_4 and kept on constant stirring in an ice bath for 30 min so that the chemicals get sufficient time to get mix with each other. Then after, 6 g of $KMnO_4$ was added slowly and gradually to the solution, the solution color immediately turned greenish black in color from black, resulting in oxidation by maintaining the temperature of the solution below 20 ^oC with constant stirring for 1 h. Then, the flask was removed from the ice bath and allowed to keep at room temperature for 4 days. After that, 92 mL boiling ultrapure water was added into the flask and followed by addition 280 mL of ultrapure water (80 ^oC) and 20 mL of 30 wt % H_2O_2 solution to terminate the reaction and kept on stirring for 15 min where dark brown color was observed in the solution. The solution was kept to settle down for overnight and was filtered to obtain the product. Solid product was washed several times with 5 wt % of HCl solution to remove impurities and sulfate ions. The product was then vacuum dried at 60 ^oC to obtain dried product as GO.

1.1.3 Synthesis of nitrogen doped sulfonated graphene nanosheet (*NS*-GNS)

Water soluble *NS*-GNS colloid was synthesized through an aryl diazonium salt coupling reaction according to previously report with small modification.[3] In a typical procedure, GO (100 mg) was dispersed in 100 mL ultrapure water, the pH of solution was adjusted by addition of 5 wt % sodium carbonate solution up to 11 and then the sample was pre-reduced with sodium borohydride ($NaBH_4$, 600 mg) at 80 °C for 1 h to synthesis partially reduced graphene oxide (p-rGO), aggregation is observed at the end of the first reduction step. After centrifuging and rinsing with ultrapure water several times, the p-rGO can be redispersed in 100 mL ultrapure water via mild sonication, then the aryl diazonium salt was added to the dispersion of p-rGO in an ice bath below 5 °C under stirring and was kept in ice bath for 5 hours to synthesis sulfonated reduced graphene oxide (*S*-rGO), aggregation was observed on the addition of the diazonium salt solution. After centrifuging and rinsing with water several times, *S*-rGO is redispersed in 100 mL ultrapure water. In the post-reduction step, 2.0 g hydrazine is added into the dispersion and the reaction mixture was kept at 90 °C for 36 h under constant stirring to get lightly *NS*-GNS. A few drops of 5 wt % sodium carbonate solution were then added into the mixture in order to precipitate the *NS*-GNS. After rinsing with water thoroughly, The *NS*-GNS thus prepared can be readily dispersed in water via a few minutes sonication. Non-dispersed impurity was removed by centrifugation at 2000 rpm for 30 min. Then, the large amount of *NS*-GNS required for the fabrication of a high concentration *NS*-GNS colloid was obtained by mixing the *NS*-GNS of several batches. The as prepared *NS*-GNS colloid was finally diluted to 1.0 $g_{NS\text{-}GNS}$ L^{-1} with ultrapure water for further investigation. Nitrogen doped graphene nanosheets (*N*-GNS) were synthesized through reducing P-rGO by hydrazine directly without treatment by the aryl diazonium salt of sulfanilic acid in an ice bath.

1.1.4 Synthesis of three dimenssional (3D) all-nanosheet RuO_2 with nitrogen doped sulfonated graphene nanosheet (RuO_2-*NS*-GNS)

The synthesis process of 3D RuO_2-*NS*-GNS complex material was as following two steps. Firstly, RuO_2 nanosheet colloid (20 mL in volume, 1.0 g_{RuO2} L^{-1} was added into *NS*-GNS colloid suspension (80 mL in volume, 1.0 $g_{NS\text{-}GNS}$ L^{-1}) dropwise under magnetic stirring for 6 h to form a stable colloidal suspension, no obvious sediment or aggregation were observed during this process. Then, the hierarchical architecture RuO_2-*NS*-GNS complex material was synthesized through a facile freeze drying the mixture of RuO_2 nanosheet and *NS*-GNS colloidal suspension for two days to remove the water completely.

1.2 Methods

1.2.1 Materials Characterization

The structure and morphology of the samples were characterized with a scanning electron microscope (FE-SEM, Hitachi S-5000) and transmission electron microscope (TEM, JEOL-JEM 2010, 200 kV). The crystal structures of the samples were analyzed using X-ray diffraction (XRD, Rigaku RINT 2500) with Cu Kα radiation. The surface topographic images of ultrathin nanosheet were obtained by tapping-mode atomic force microscopy (AFM, SPA400, Seiko instruments) with Si-tip cantilever (20 N m^{-1}). Raman measurements were carried out at room temperature in backscattering geometry with a LabRam HR800 UV spectrometer operating with a 488 nm laser. X-ray photoelectron spectroscopy (XPS) was performed on a Kratos Ultra AXIS Spectrometer system equipped with a monochromatic Mg-Kα source (15 kV). ^{1}H nuclear magnetic resonance (NMR) spectra were collected on a Varian 400 MR spectrometer. The samples were extracted by soaking the discharge or recharge electrode in D_2O containing 0.05 wt% 3-(trimethylsilyl)propionic-2,2,3,3-d^4 acid with sodium salt (99.9 atom% D, SigmaAldrich) in the glovebox.

1.2.2 Electrode preparation

Electrode slurry was prepared by mixing as-prepared complex materials and nafion solution (Sigma Aldrich). The mixture was then coated onto a carbon fiber paper (Toray Carbon Paper, TGP-H-060) followed by drying at 80 °C in a vacuum oven for 24 h. The electrode was then cut into circular discs with a diameter of 12 mm. The mass loading of the catalyst was 0.6-0.8 mg cm^{-2} for each disc.

1.2.3 Battery Assemble and Electrochemical Characterization

Nonaqueous Li-O_2 battery: The nanoaqueous Li-O_2 batteries were assembled in the argon filled glove box with oxygen and water contents less than 1 ppm. The battery consists of high-purity metallic lithium foil anode, a glass microfiber filter (GF/A, Whatman), electrolyte of 1 mol L^{-1} lithium trifluoromethanesulfonate/tetraethylene glycol dimethyl ether (LiTFSI/TEGDME), and RuO_2-*NS*-GNS as cathode. For comparison, Li-O_2 batteries with *N*-GNS or *NS*-GNS were also prepared in the same process. Galvanostatic discharge/charge tests of nonaqueous Li-O_2 batteries were carried out on a Biologic VMP3 battery test system at 25 °C or the batteries were discharge/charge at a fixed specific capacity limitation of 1000 mAh g^{-1}.

Aqueous Li-O_2 battery: Aqueous Li-O_2 batteries were constructed by air cathode, aqueous electrolyte and a multilayer water-stable lithium electrode as we described previously.[4,5] The water-stable lithium electrode was assembled by laminating the lithium metal, $PEO_{18}LiTFSI$-10wt % $BaTiO_3$ and water-proof lithium ion conductor $Li_{1+x+y}Ti_{2-x}Al_xSi_yP_{3-y}O_{12}$ (LTAP) plate in a plastic aluminum film package, leaving a square window of 0.5×0.5 cm^2 on one side. 1.0 M LiOH-5.0 M $LiNO_3$ aqueous solution was selected as the aqueous electrolyte by optimizing the pH and conductivity of LiOH-$LiNO_3$-H_2O system, and the as-prepared catalyst loading on carbon fiber paper as the cathode. Galvanostatic discharge/charge measurements were carried out using a beaker cell at 60 ºC and a limited specific capacity of 1000 mA g^{-1} at 50 mA g^{-1} (based on the activate material, corresponding to 0.15 mA cm^{-2}), the aqueous electrolyte was purged with O_2 gas for 30 min with a small gas tube into the solution before electrochemical measurement.

1.2.4 Calibration of reference electrode to reversible hydrogen electrode (RHE)

The calibration of Hg/HgO electrode was performed in a standard three-electrode system with polished Pt rotating disk electrode as the working electrode, Pt mesh as counter electrode and the Hg/HgO/1M NaOH electrode as the reference electrode.[6] 1.0 M LiOH-5.0 M $LiNO_3$ electrolyte is pre-purged and saturated with high purity H_2. Linear scanning voltammetry (LSV) is then run at a scan rate of 0.5 mV s^{-1} with a rotating speeding 1200 rpm, and the potential at which the current crossed zero was taken to be the thermodynamic potential for the hydrogen electrode reaction.

1.2.5 Impedance resistance (*iR*) compensation

IR calibration of glass carbon electrode was measured in O_2 purging 1.0 M LiOH-5.0 M $LiNO_3$ electrolyte with amplitude 5 mV. Pt mesh was used as counter electrode and Hg/HgO/1M NaOH was used as reference electrode.[7]

1.3 Supporting Results

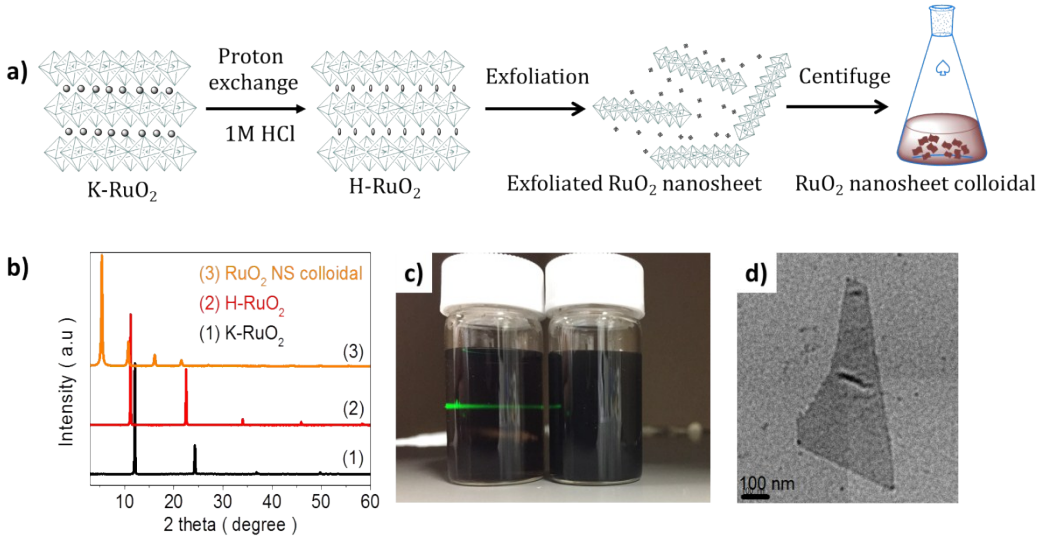

Figure S1：(a) Schematic illustration of the fabrication process of RuO_2 nanosheet; (b) XRD patterns of the layered K-RuO_2, H-RuO_2 and restacked RuO_2 nanosheet; (c) Photograph of a colloidal suspension of RuO_2 nanosheets with low concentration (left) and high concentration (right), the light beam is incident from the side to demonstrate the Tyndall effect; (d) TEM image of monolayer RuO_2 nanosheet.

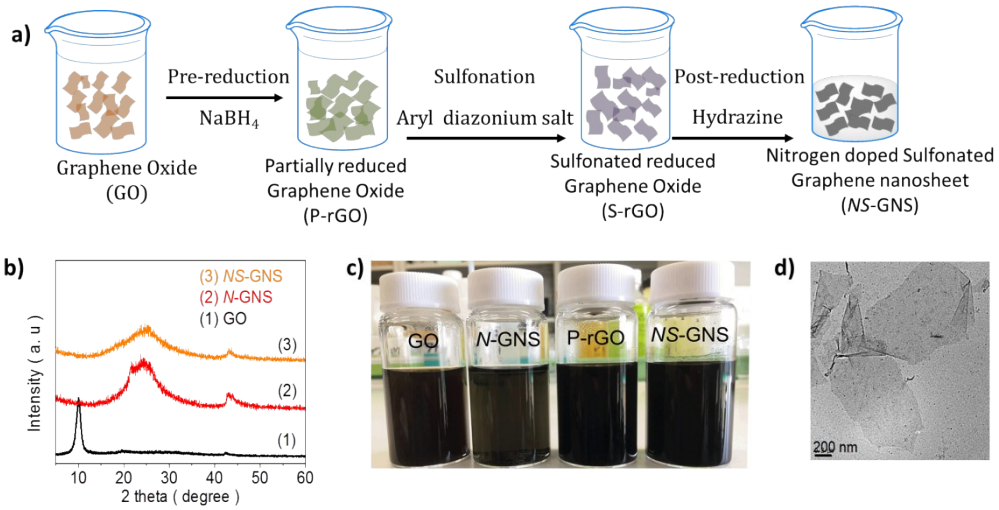

Figure S2: (a) Schematic illustration of the fabrication process of *NS*-GNS; (b) XRD patterns of graphite, *N*-GNS and *NS*-GNS; (c) Photograph of GO, *N*-GNS, P-rGO and *NS*-GNS, there are a lot of insoluble precipitant for *N*-GNS because the absence of p-phenyl-SO3H groups; [3] (d) TEM image of monolayer *NS*-GNS.

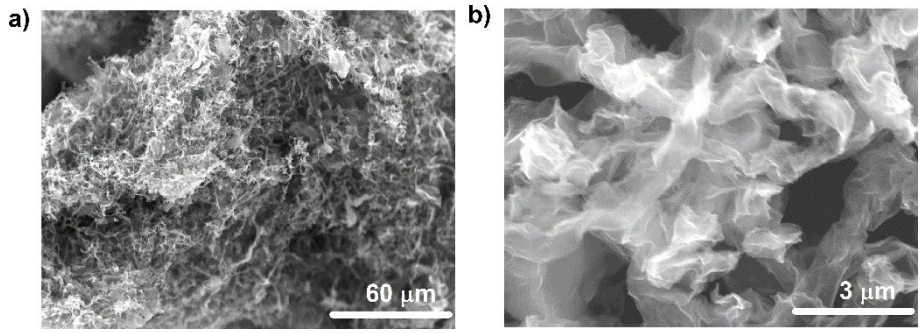

Figure S3: Microstructure of RuO_2-*NS*-GNS after freeze drying with (a) low magnification and (b) high magnification.

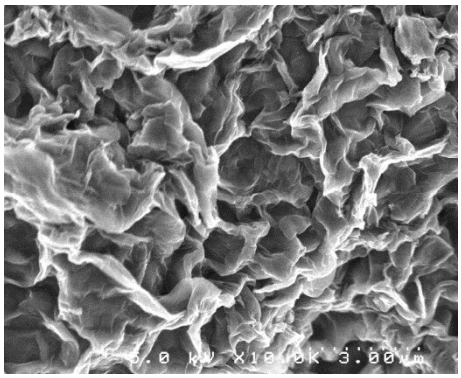

Figure S4: Microstructure of *NS*-GNS after freeze drying, which is different from the morphology of RuO_2-*NS*-GNS.

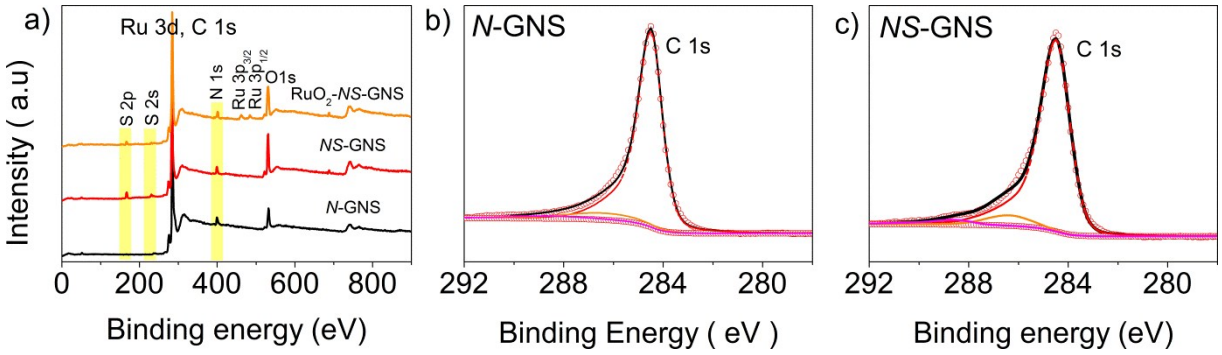

Figure S5: XPS survey and C1s spectra of *N*-GNS, *NS*-GNS and RuO_2-*NS*-GNS.

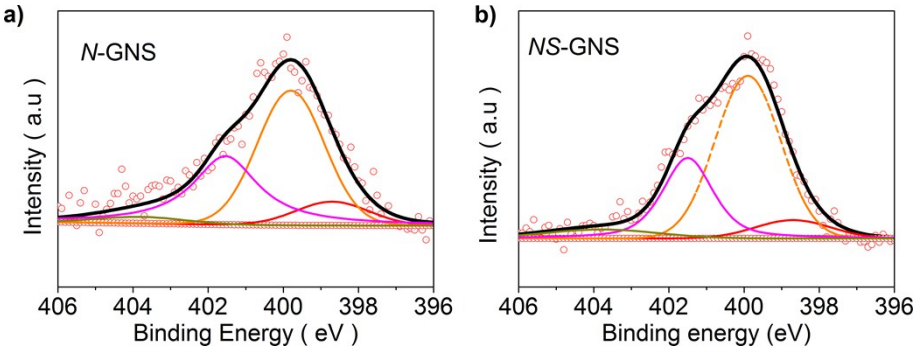

Figure S6: Deconvoluted N1s spectra of *N*-GNS and *NS*-GNS. There are four nitrogen species (pyridinic N at 398.5-398.8 eV, pyrrolic N at 399.9-400.2 eV, quaternary N at 401.4-401.6 eV and N-oxide at 403.7-404.2 eV in each as-prepared catalyst.[8-10]

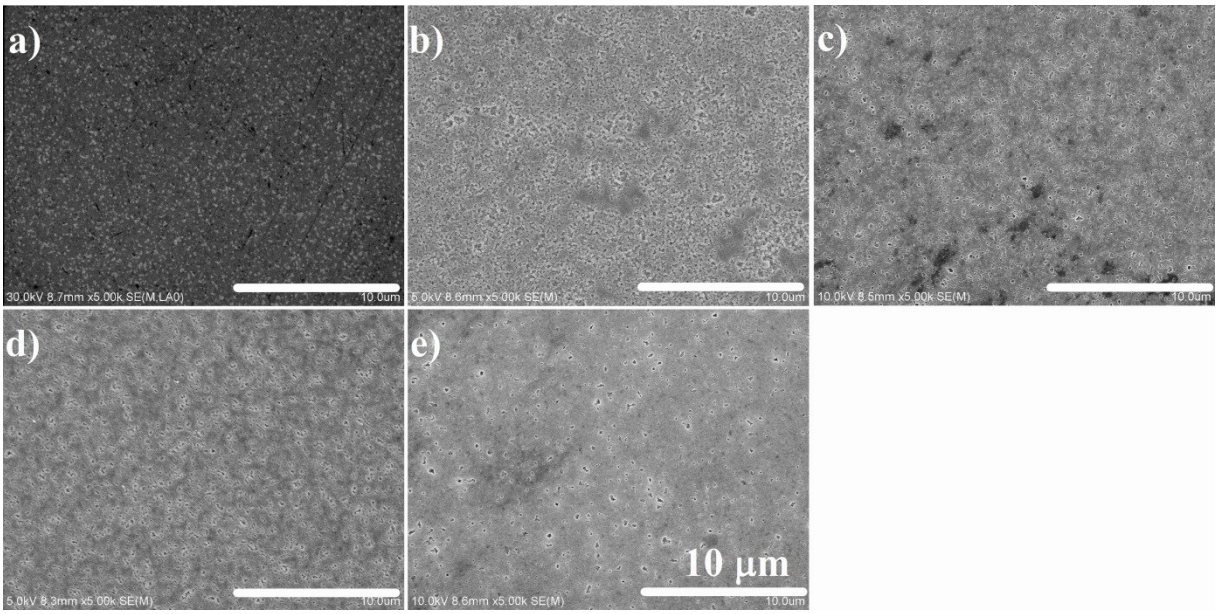

Figure S7: SEM images of LTAP glass ceramic after soaked in LiOH-$LiNO_3$-H_2O aqueous solution system at room temperature for 15 days. (a) Pristine LTAP and LTAP soaked in (b) 1 M LiOH and 1 M $LiNO_3$ solution; (c) 1 M LiOH and 2 M $LiNO_3$ solution; (d) 1 M LiOH and 5 M $LiNO_3$ solution; (e) 1 M LiOH and 10 M $LiNO_3$ solution.

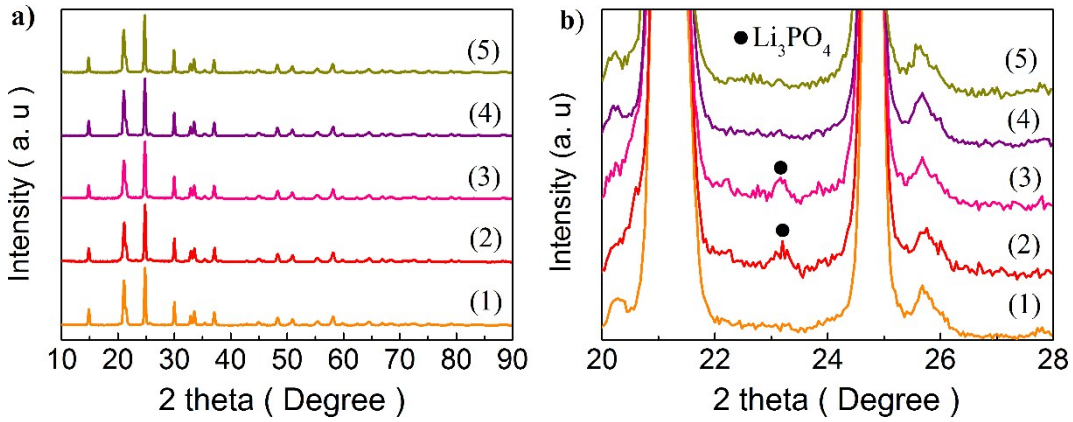

Figure S8: XRD patterns of LTAP glass ceramic after soaked in LiOH-$LiNO_3$-H_2O system at room temperature for 15 days. (1) Pristine LTAP and LTAP soaked in (2) 1 M LiOH and 1 M $LiNO_3$ solution; (3) 1 M LiOH and 2 M $LiNO_3$ solution; (4) 1 M LiOH and 5 M $LiNO_3$ solution; (5) 1 M LiOH and 10 M $LiNO_3$ solution.

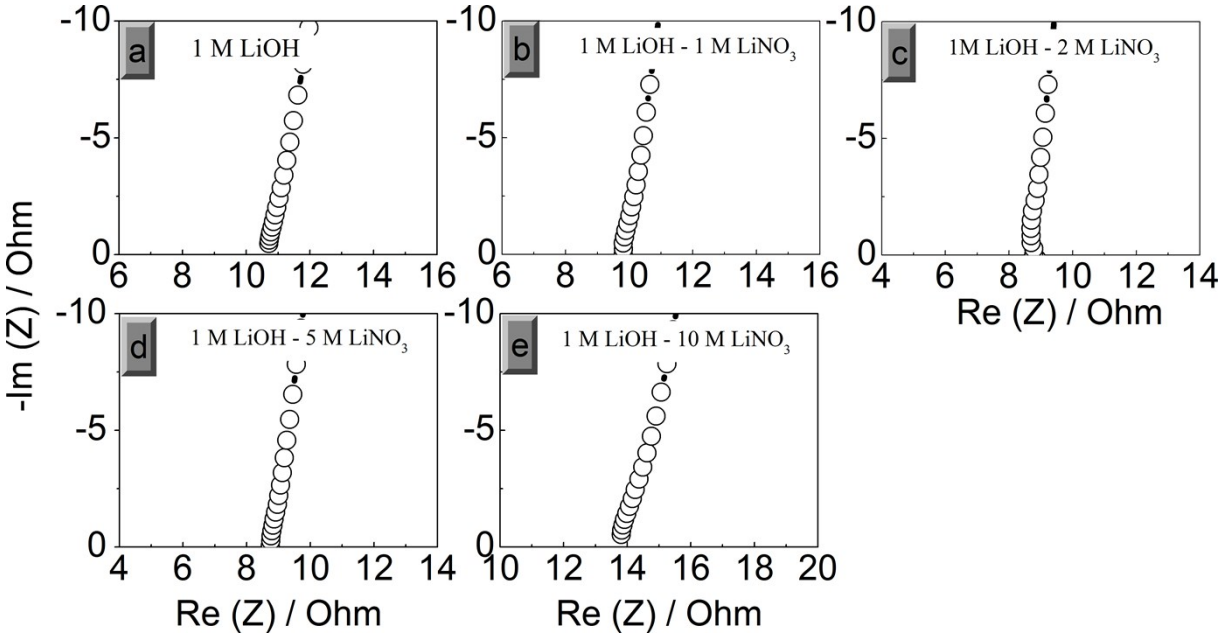

Figure S9: Impedance resistance calibration of glass carbon electrode in O_2 purging LiOH-$LiNO_3$-H_2O system with amplitude 5mV. Pt wire was used as counter electrode and Hg/HgO/1M NaOH was used as reference electrode. The resistance values of aqueous electrolyte LiOH-$LiNO_3$-H_2O system decrease with increasing content of $LiNO_3$ untill 1M LiOH and 5M $LINO_3$ solution, and then turns into increase with 1M LiOH and 10M $LiNO_3$, the change maybe cause by viscosity and ionic concentration.

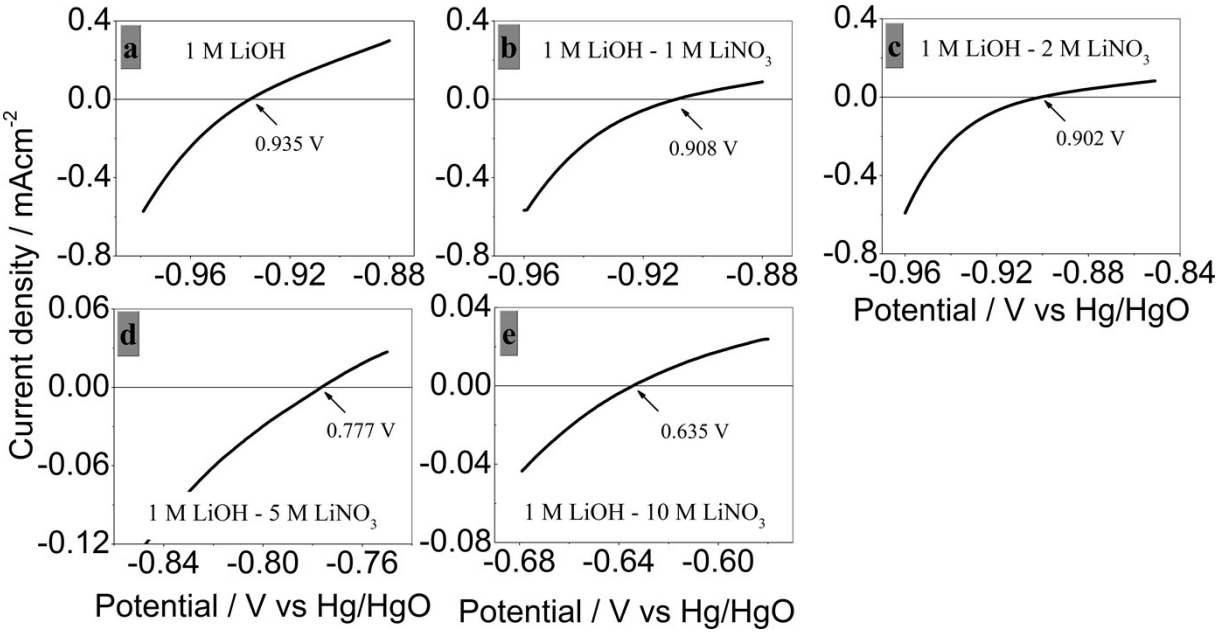

Figure S10: Calibration of reversible hydrogen electrode (RHE) in LiOH-$LiNO_3$-H_2O system.

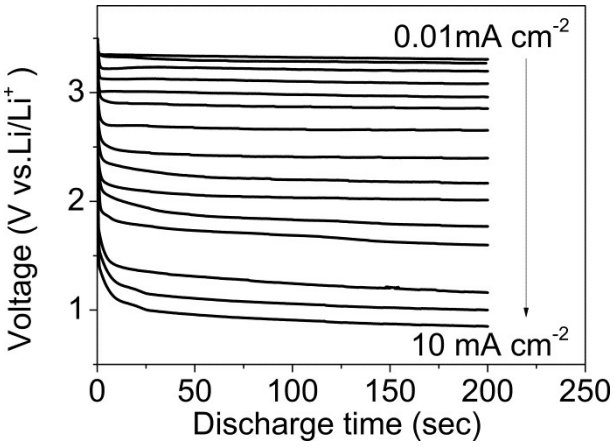

Figure S11: The polarization curves of the aqueous Li-O_2 battery with RuO_2-*NS*-GNS electrode at various current densities for 200 s.

1.4 Supporting tables

Table S1: Elemental compositions calculated from the XPS data and I_D/I_G value calculated from Raman spectrum of *N*-GNS, *NS*-GNS and RuO_2-*NS*-GNS.

Sample	C (wt. %)	O (wt. %)	N (wt. %)	S (wt. %)	Ru (wt. %)	I_D/I_G
N-GNS	81.38	15.04	3.58	0	0	1.49
NS-GNS	78.90	14.63	3.07	3.41	0	1.42
RuO_2-*NS*-GNS	74.73	13.31	2.49	2.48	7.00	1.35

Table S2: XPS quantitative analysis of four nitrogen species (pyridinic N at 398.5-398.8 eV, pyrrolic N at 399.9-400.2 eV, quaternary N at 401.4-401.6 eV and N-oxide at 403.7-404.2 eV) from the deconvoluted N 1s spectra of as-synthesized *N*-GNS, *NS*-GNS and RuO_2-*NS*-GNS.

Sample	N-oxide (wt. %)	Quaternary N (wt. %)	Pyrrolic N (wt. %)	Pyridinic N (wt. %)
N-GNS	3.3	27.1	61.7	7.9
NS-GNS	2.8	26.3	63.1	7.8
RuO_2-*NS*-GNS	0.7	78.6	4.7	16.0

Table S3: Physical and electrochemical properities of $LiOH$-$LiNO_3$-H_2O system. The pH values of the system do not depend on the concentration of LiOH, but monotonously decrease with increasing content of $LiNO_3$, suggesting that excess amount of Li^+ ions can restrain the dissociation of LiOH to Li^+ and OH^-.

Electrolyte	pH	RHE Calibration Equation	*iR* Calibration (Ω)
1M LiOH	12.35	$E_{RHE} = E_{Hg/HgO} + 0.935$ V	10.50
1 M LiOH - 1 M $LiNO_3$	11.83	$E_{RHE} = E_{Hg/HgO} + 0.908$ V	9.81
1 M LiOH - 2 M $LiNO_3$	11.49	$E_{RHE} = E_{Hg/HgO} + 0.902$ V	8.79
1 M LiOH - 5 M $LiNO_3$	10.68	$E_{RHE} = E_{Hg/HgO} + 0.777$ V	8.73
1 M LiOH - 10 M $LiNO_3$	9.62	$E_{RHE} = E_{Hg/HgO} + 0.635$ V	13.81

1.5 References

[1] W. Sugimoto, H. Iwata, Y. Yasunaga, Y. Murakami, Y. Takasu, *Angew. Chem. Int. Ed.*, 2003, **42**, 4092-4096.

[2] J. William, S. Hummers, R. E. Offeman, J. Am. Chem. Soc., 1958, **80**, 1339-1339.

[3] Y. C. Si, E. T. Samulski, *Nano Lett.,* 2008, **8**, 1679-1682.

[4] M. Zhang, K. Takahashi, I. Uechi, Y. Takeda, O. Yamamoto, D. M. Im, D. J. Lee, B. Chi, J. Pu, J. Li, N. Imanishi, *J. Power Sources*, 2013, **235**, 117-121.

[5] H. Wang, D. Im, D. J. Lee, M. Matsuia, Y. Takeda, O. Yamamoto, N. Imanishi, *J. Electrochem. Soc.*, 2013, **160**, A728-A733.

[6] Y. Y. Liang, Y. G. Li, H. L.Wang, J. G. Zhou, J. Wang, T. Regier, H. J. Dai, *Nat. Mater.*, 2011, **10**, 780-786.

[7] Y. Lee, J. Suntivich, K. J. May, E. E. Perry, Y. Shao-Horn, *J. Phys. Chem. Lett.*, 2012, **3**, 399-404.

[8] H. J. Huang, J. X. Zhu, W. Y. Zhang, C. S. Tiwary, J. F. Zhang, X. Zhang, Q. G. Jiang, H. Y. He, Y. P. Wu, W. Huang, P. M. Ajayan, Q. Y. Yan, *Chem. Mater.*, 2016, **28**, 1737-1745.

[9] K. P. Gong, F. Du, Z. H. Xia, M. Durstock, L. M. Dai, *Science*, 2009, **323**, 760-764.

[10] J. Y. Xu, Y. H. Kan, R. Huang, B. S. Zhang, B. L. Wang, K. H. Wu, Y. M. Lin, X. Y. Sun, Q. F. Li, G. Centi, D. S. Su, *ChemSusChem*, 2016, **9**, 1085-1089.